This Accepted Manuscript has not been copyedited and formatted. The final version may differ from this version.

JNeurosci
THE JOURNAL OF NEUROSCIENCE

Research Articles: Neurobiology of Disease

Evidence for compartmentalized axonal mitochondrial biogenesis: Mitochondrial DNA replication increases in distal axons as an early response to Parkinson's disease-relevant stress

Victor S. Van Laar[1,2], Beth Arnold[1,2], Evan H. Howlett[1,2], Michael J. Calderon[3,4], Claudette M. St. Croix[3,4], J. Timothy Greenamyre[1,2], Laurie H. Sanders[1,2,5] and Sarah B. Berman[1,2]

[1]*University of Pittsburgh Department of Neurology, University of Pittsburgh, Pittsburgh PA, 15213*
[2]*The Pittsburgh Institute for Neurodegenerative Diseases, University of Pittsburgh, Pittsburgh PA, 15213*
[3]*Department of Cell Biology, University of Pittsburgh, Pittsburgh PA, 15261*
[4]*The Center for Biologic Imaging, University of Pittsburgh, Pittsburgh PA, 15261*
[5]*Department of Neurology, Duke University Medical Center, Durham NC, 27710*

DOI: 10.1523/JNEUROSCI.0541-18.2018

Received: 26 February 2018

Revised: 19 June 2018

Accepted: 7 July 2018

Published: 20 July 2018

Author contributions: V.S.V., B.A.A., E.H.H., M.J.C., C.M.S.C., T.G., L.H.S., and S.B.B. designed research; V.S.V., B.A.A., E.H.H., M.J.C., C.M.S.C., L.H.S., and S.B.B. performed research; V.S.V., B.A.A., E.H.H., M.J.C., C.M.S.C., T.G., L.H.S., and S.B.B. analyzed data; V.S.V. and S.B.B. wrote the first draft of the paper; V.S.V., B.A.A., E.H.H., M.J.C., C.M.S.C., T.G., L.H.S., and S.B.B. edited the paper.

Conflict of Interest: The authors declare no competing financial interests.

This work was supported by a grant from the NIH (R01NS077954, S.B.B.), a University of Pittsburgh Physicians Academic Foundation Research Grant (S.B.B), the DSF Charitable Foundation, and the William N. & Bernice E. Bumpus Foundation Innovation Award (L.H.S.). We also wish to thank Simon Watkins and Mads Larsen of the University of Pittsburgh Center for Biologic Imaging for their imaging expertise and assistance during these studies.

Correspondence should be addressed to CORRESPONDING AUTHOR: Sarah B. Berman, M.D., Ph.D., Associate Professor, Department of Neurology, Pittsburgh Institute for Neurodegenerative Diseases, University of Pittsburgh, Biomedical Science Tower 3, 7037, 3501 Fifth Avenue, Pittsburgh, PA 15213, Phone: (412) 383-5868, email: bermans@upmc.edu

Cite as: J. Neurosci ; 10.1523/JNEUROSCI.0541-18.2018

Alerts: Sign up at www.jneurosci.org/cgi/alerts to receive customized email alerts when the fully formatted version of this article is published.

Accepted manuscripts are peer-reviewed but have not been through the copyediting, formatting, or proofreading process.

Copyright © 2018 the authors

JNeurosci Accepted Manuscript

JNeurosci Accepted Manuscript

TITLE

Evidence for compartmentalized axonal mitochondrial biogenesis: Mitochondrial DNA replication increases in distal axons as an early response to Parkinson's disease-relevant stress

ABBREVIATED TITLE

Rotenone increases axonal mitochondrial biogenesis

AUTHORS & AFFILIATIONS

Victor S. Van Laar[1,2], Beth Arnold[1,2], Evan H. Howlett[1,2], Michael J. Calderon[3,4], Claudette M. St. Croix[3,4], J. Timothy Greenamyre[1,2], Laurie H. Sanders[1,2,5], and Sarah B. Berman[1,2]

[1]University of Pittsburgh Department of Neurology, University of Pittsburgh, Pittsburgh PA, 15213
[2]The Pittsburgh Institute for Neurodegenerative Diseases, University of Pittsburgh, Pittsburgh PA, 15213
[3]Department of Cell Biology, University of Pittsburgh, Pittsburgh PA, 15261
[4]The Center for Biologic Imaging, University of Pittsburgh, Pittsburgh PA, 15261
[5]Department of Neurology, Duke University Medical Center, Durham NC, 27710

CORRESPONDING AUTHOR

Sarah B. Berman, M.D., Ph.D.
Associate Professor, Department of Neurology
Pittsburgh Institute for Neurodegenerative Diseases
University of Pittsburgh
Biomedical Science Tower 3, 7037
3501 Fifth Avenue, Pittsburgh, PA 15213

Phone: (412) 383-5868
email: bermans@upmc.edu

NUMBER OF PAGES: **33**

NUMBER OF FIGURES: **6**

ABSTRACT: **247 words**

INTRODUCTION: **650 words**

DISCUSSION: **1,297 words**

CONFLICT OF INTEREST: **None**

ACKNOWLEDGEMENTS:

This work was supported by a grant from the NIH (R01NS077954, S.B.B.), a University of Pittsburgh Physicians Academic Foundation Research Grant (S.B.B), the DSF Charitable Foundation, and the William N. & Bernice E. Bumpus Foundation Innovation Award (L.H.S.). We also wish to thank Simon Watkins and Mads Larsen of the University of Pittsburgh Center for Biologic Imaging for their imaging expertise and assistance during these studies.

JNeurosci Accepted Manuscript

ABSTRACT

Dysregulation of mitochondrial biogenesis is implicated in the pathogenesis of neurodegenerative diseases such as Parkinson's disease (PD). However, it is not clear how mitochondrial biogenesis is regulated in neurons, with their unique compartmentalized anatomy and energetic demands. This is particularly relevant in PD, since selectively vulnerable neurons feature long, highly arborized axons where degeneration initiates. We previously found that exposure of neurons to chronic, sublethal doses of rotenone, a Complex I inhibitor linked to PD, causes early increases in mitochondrial density specifically in distal axons, suggesting possible upregulation of mitochondrial biogenesis within axons. Here, we directly evaluated for evidence of mitochondrial biogenesis in distal axons and examined whether PD-relevant stress causes compartmentalized alterations. Utilizing BrdU labeling and imaging to quantify replicating mitochondrial DNA (mtDNA) in primary rat neurons (pooled from both sexes), we provide evidence of mtDNA replication in axons along with cell bodies and proximal dendrites. We found that exposure to chronic, sublethal rotenone increases mtDNA replication first in neurites, later extending to cell bodies, complementing our mitochondrial density data. Further, isolating axons from cell bodies and dendrites, we discovered that rotenone exposure upregulates mtDNA replication in distal axons. Utilizing super-resolution stimulated emission depletion (STED) imaging, we identified mtDNA replication at sites of mitochondrial-endoplasmic reticulum contacts in axons. Our evidence suggests mitochondrial biogenesis occurs not only in cell bodies, but also in distal axons, and is altered under PD-relevant stress conditions in an anatomically compartmentalized manner. We hypothesize that this contributes to vulnerability in neurodegenerative diseases.

JNeurosci Accepted Manuscript

SIGNIFICANCE STATEMENT

Mitochondrial biogenesis is crucial for maintaining mitochondrial and cellular health and has been linked to neurodegenerative disease pathogenesis. However, regulation of this process is poorly understood in central nervous system (CNS) neurons, which rely on mitochondrial function for survival. Our findings offer fundamental insight into these regulatory mechanisms by demonstrating that replication of mitochondrial DNA, an essential precursor for biogenesis, can occur in distal regions of CNS neuron axons, independent of the soma. Further, this process is upregulated specifically in axons as an early response to neurodegeneration-relevant stress. This is the first demonstration of the compartmentalized regulation of CNS neuronal mitochondrial biogenesis in response to stress, and may prove a useful target in development of therapeutic strategies for neurodegenerative disease.

JNeurosci Accepted Manuscript

INTRODUCTION

Neurons are dependent on mitochondria for survival and function, and mitochondrial homeostasis is maintained via regulated fission, fusion, active transport, degradation, and biogenesis, collectively termed mitochondrial dynamics (Detmer and Chan, 2007). Together, these dynamic processes regulate mitochondrial DNA (mtDNA) stability, mitochondrial turnover, cell death mechanisms, and proper distribution of mitochondria to synapses (Detmer and Chan, 2007). Disruption of mitochondrial dynamics is detrimental to neuronal survival and has been increasingly implicated in the pathogenesis of neurodegenerative diseases such as Parkinson disease (PD) (Van Laar and Berman, 2009 and 2013; McCoy and Cookson, 2012; Bose and Beal, 2016).

In PD, mitochondrial biogenesis may be the important link between dysregulation of mitochondrial homeostasis and neurodegeneration. Mitochondrial biogenesis is a complex process, involving mtDNA replication, coordinated gene expression, protein synthesis, membrane formation, and mitochondrial division (Nisoli et al., 2004). The degenerative process in PD is thought to begin in distal axons of vulnerable neurons (Braak et al., 2004), which feature long, poorly myelinated, and highly-branched axons with high ATP requirements (Braak et al., 2004; Surmeier et al., 2017). Mitochondrial biogenesis is likely to be critical in these distal, highly energy-requiring regions, and growing evidence implicates dysregulation of mitochondrial biogenesis in PD. For example, it was discovered that neurodegeneration caused by mutations in the familial PD genes, *PINK1* and *parkin*, is due in part to suppression of activity of the 'master mitochondrial biogenesis regulator', transcription coactivator PPAR gamma-coactivator 1 alpha (PGC1α) (Stevens et al., 2015; Lee et al., 2017). In addition, overexpression of familial PD gene *alpha-synuclein* causes neurodegeneration in zebrafish that is

JNeurosci Accepted Manuscript

prevented by upregulating PGC1α expression (O'Donnell et al., 2014), further implicating a critical role for biogenesis in PD.

Neurons, especially those in the central nervous system (CNS), have unique anatomical and functional characteristics, with extended axons and arborization. Yet it is not known whether regulation of mitochondrial biogenesis takes place throughout this extended arborization. In our previous work, we studied early changes in mitochondrial dynamics in CNS neurons in a chronic PD-relevant toxicant model (Arnold et al., 2011). Unexpectedly, we discovered that mitochondrial density in distal axons increased early after chronic nonlethal rotenone exposure, without a concomitant increase inside cell bodies. However, the axonal mitochondrial density changes could not be explained by alterations in mitochondrial axonal transport, nor did we find evidence of decreased mitochondrial degradation (Arnold et al., 2011). Thus, the mitochondrial increase exclusively in axons suggests an unconventional hypothesis: that mitochondrial biogenesis can occur in distinct, anatomically compartmentalized distal axons. It also suggests that compartmentalized biogenesis may increase as an early response to chronic neurotoxic PD-relevant stress, specifically in distal axonal regions where neurodegeneration starts.

It is generally presumed that mitochondrial biogenesis takes place exclusively in cell bodies, near nuclear machinery for protein translation, with new mitochondria transported down axons (Davis and Clayton, 1996; Li et al., 2017). However, for post-mitotic neurons with long, branched axons, this seems an inadequate means of replacing dysfunctional mitochondria at synaptic terminals. It is known that mRNA of mitochondrially-targeted proteins can be transported down axons, and that translation of these mRNA are essential for maintaining axonal mitochondrial function (Gioio et al., 2001; Hillefors et al., 2007; Kar et al., 2014). Evidence of mtDNA replication in proximal neurites of peripheral neurons

JNeurosci Accepted Manuscript

has been reported (Amiri and Hollenbeck, 2008; Lentz et al., 2010), but evidence for distal axonal biogenesis in CNS neurons has never been described, nor have distinct, compartmentalized alterations under CNS disease-relevant conditions.

Therefore, we investigated these fundamental questions, testing the hypothesis that mitochondrial biogenesis in CNS neurons is not limited to cell bodies but also occurs in distal axons. We then evaluated for evidence of anatomic compartmentalization of mitochondrial biogenesis, investigating whether biogenesis increases in distal axons in response to chronic neurotoxic PD-relevant stress, distinct from, and prior to, changes in cell body mitochondrial biogenesis. Our findings provide evidence for mitochondrial biogenesis in distal axons, with early upregulation in response to PD-relevant stress.

JNeurosci Accepted Manuscript

METHODS

Primary Neuron Culture and Treatment

Primary cortical neurons were cultured as previously described (Arnold et al., 2011). Briefly, neurons were derived from E18 Sprague Dawley rats (pooled from both male and female embryos), and plated in serum-containing Neurobasal medium at a density of 3 x 10^5cells/ml on glass coverslips coated with poly-D-lysine and mouse laminin. Media was replaced with serum-free Neurobasal media, and ½ media was changed every 3-4d. Treatments with 1nM rotenone or DMSO vehicle were initiated at DIV7, and continued with regular feedings for 1-2wk. For microfluidic device culture, standard 2-chamber microfluidic neuron devices with a 450µm- or 900µm-width microgroove barrier (Xona microfluidics) were placed on coverslips coated with poly-D-lysine. Neurons were plated in the cell body chamber at 50,000 cells per device. After plating, no media changes occurred until the initial treatment with 1nM rotenone or DMSO vehicle control at DIV7, with a ½ media change in both the axonal and cell body chambers. Treatments continued with ½ media changes every 3-4d.

Transfection of Cortical Neurons

Cells were transfected on DIV6 using Lipofectamine 2000 as previously described (Arnold et al., 2011). Briefly, cell culture media was saved and exchanged for Transfection/Incubation Media (MEM pH 7.4, 2% glutamax, 20 mM HEPES, 33 mM glucose, 1mM Na-pyruvate; Thermo Fisher). Cells were incubated with Transfection Media at 37°C in a non-CO2 incubator for 1.5hr, and then media was replaced. Neurons were transfected where noted with plasmids expressing mitochondrially-targeted DsRed2 (mtDsRed2; Clontech), mitochondrially-targeted photo-activatable GFP (PA-mtGFP; (Karbowski et al.,

JNeurosci Accepted Manuscript

2004)), and/or green fluorescent protein-tagged endoplasmic reticulum protein Sec61β (GFP-Sec61β; Addgene plasmid 15108; deposited by T. Rapoport (Voeltz et al., 2006)). Of note, we routinely obtain 100% co-transfection with multiple plasmids (Arnold et al., 2011).

BrdU and EdU Detection and Immunocytochemistry

At the specified time points and/or following chronic rotenone or DMSO vehicle control treatments, cells were treated with either 5-bromo-2'-deoxyuridine (BrdU, 10μM; Sigma) or 5-ethynyl-2'-deoxyuridine (EdU, 10μM; Sigma) for the indicated length of time. For negative controls, DMSO vehicle control cells either were not treated with thymidine analogs, or were pre-treated for 6hr with 100μM 2',3'-dideoxycytidine (ddC) followed by co-treatment of ddC and thymidine analog. Immediately following BrdU or EdU exposure, cells were rinsed with PBS, then fixed using 4% PFA at RT for 20 min. For BrdU detection, cells were permeabilized in 0.5% Triton X-100 in PBS on ice for 5 min, then treated with 2N HCl for 30min at RT to denature the DNA, and rinsed with PBS. Cells then underwent sequential fluorescent immunocytochemical staining. Cells were first stained for BrdU (mouse anti-BrdU, 1:1000, BD Pharmingen 555627). Briefly, cells were blocked in normal donkey serum for 30min, then incubated with BrdU primary overnight at 4°C, followed by 1hr incubation with secondary (donkey anti-mouse Alexa 488, 1:500, ThermoFisher; donkey anti-mouse Alexa 555, 1:500, ThermoFisher). Cells were then rinsed in PBS and incubated with either MAP2 (rabbit anti-MAP2, 1:1000, Millipore ab5622) or mitochondrial SSBP (rabbit anti-mtSSBP, 1:2000, Origene TA314569) primaries again overnight at 4°C, followed by 1hr incubation with secondary (donkey anti-rabbit Cy3, 1:500, Jackson Immunology; donkey anti-rabbit 647, 1:500, ThermoFisher). Coverslips were rinsed in PBS followed by ddH_2O and mounted onto slides using gelvatol mounting media. For experiments utilizing neurons transfected with PA-mtGFP, BrdU immunochemical detection and mounting was

JNeurosci Accepted Manuscript

101 performed as described above. PA-mtGFP in fixed neurons was photoactivated via brief exposure to
102 405nm laser as previously described (Berman et al., 2009), which increases GFP fluorescence of this
103 protein 100-fold when excited at 488 nm (Karbowski et al., 2004). The photoactivatable fluorescence
104 property of PA-mtGFP was unaffected by acid treatment as evidenced by robust green fluorescence in
105 mitochondria after activation (see Figures 1 A-D). For EdU detection, fixed cells were stained using the
106 EdU Click-iT Alexa Fluor 647 kit from ThermoFisher per manufacturer's instructions and mounted on
107 slides using ProLong Gold mounting media (ThermoFisher).
108
109 For immunocytochemical detection of equilibrative nucleoside transporter 1 (ENT-1), neurons were
110 cultured on microfluidic devices and transfected on DIV7 to express mitochondrially-targeted
111 mtDsRed2. Cell were fixed on DIV14, and immunocytochemistry was performed using rabbit anti-ENT-
112 1 (1:100; Alomone ANT-051) primary overnight at 4°C, followed by 1hr incubation with secondary
113 (donkey anti-rabbit Cy3, 1:500, Jackson Immunology). Cells were rinsed in PBS and mounted using
114 ProLong Gold mounting media (ThermoFisher).
115
116 For immunocytochemical detection of COXIV, neurons cultured on microfluidic devices were treated
117 with DMSO vehicle control or 1nM rotenone for 1 week as described above. After fixation,
118 immunocytochemistry was performed using mouse anti-COXIV (1:1,000; Abcam ab14744) primary
119 overnight at 4°C, followed by 1hr incubation with secondary (donkey anti-mouse Alexa 555, 1:500,
120 ThermoFisher). To detect actin, cells were then incubated with 165nM AlexaFluor 488 Phalloidin
121 (Thermo Fisher) for 20 minutes at RT followed by PBS wash and then mounted using ProLong Gold
122 mounting media (ThermoFisher).
123

JNeurosci Accepted Manuscript

BrdU Imaging and Analyses

All images for assessing BrdU incorporation were acquired using an Olympus IX81 inverted microscope with a FV1000 laser scanning confocal system with a 60x 1.42NA oil-immersion objective. To assess BrdU in neurons cultured on coverslips, image stacks were taken at 1024x1024 pixel resolution (0.207µm/pixel) with 0.50µm z-steps. To assess BrdU in neurons grown in microfluidic devices, image stacks of random fields of distal axons on the axon chamber side were taken at 1024x1024 pixel resolution with 0.25µm z-steps, and random fields of cell bodies on the cell body chamber side of the device were taken at 1024x1024 pixel resolution with 0.50µm z-steps. After acquisition, images were analyzed using the Fiji distribution of ImageJ (Schindelin et al., 2012; Schneider et al., 2012). BrdU detection in image fields from experimental groups was thresholded to fields taken from negative control cells not exposed to BrdU, using Fiji Color Threshold (using Brightness). For BrdU puncta analysis, cell bodies were first identified and outlined as regions of interest (ROIs). Fiji Particle Analysis with size limit set to 0-5 pixels was then used to count the number of BrdU puncta either within ROIs (e.g., in cell bodies; represented as "puncta per cell") or outside the ROIs (e.g., in neuritic processes; represented as "puncta in processes per field").

COXIV Imaging and Analyses

For experiments assessing COXIV protein levels via quantitative immunofluorescence, all images were acquired using an Olympus IX81 inverted microscope with a FV1000 laser scanning confocal system using a 60x 1.42NA oil-immersion objective at 2X magnification and 1024x1024 pixel resolution (0.103µm/pixel). Vehicle control- or rotenone-treated neuronal cultures grown on microfluidic devices were stained and mounted as described above. Cells were imaged using identical laser and detector

JNeurosci Accepted Manuscript

147 settings across devices within an experiment for both control and rotenone conditions. For axon
148 imaging, random fields of axons on the axon chamber side of the device were imaged with 0.25µm z-
149 steps. Similarly, random fields of cell bodies on the cell body chamber side of the device were imaged
150 with 0.50µm z-steps. For COXIV intensity quantification in axons, image analysis was done using Nikon
151 Elements. 3D spot detection was used to characterize individual mitochondria, and 3D thresholding
152 was used to measure actin volume. Identical threshold settings for COXIV fluorescence intensity were
153 utilized for control- and rotenone-treated conditions within each experiment. Only COXIV-positive
154 puncta colocalizing with actin were used for analysis. Data are reported as COXIV intensity normalized
155 to actin volume. For COXIV intensity quantification in the soma, individual neuronal cell bodies were
156 outlined as regions of interest (ROIs) and the total intensity and area of each cell body was assessed
157 using Olympus FV10-ASW Version 4.06 software. Data are reported as COXIV intensity normalized to
158 ROI area.
159
160 *Western Blot Analyses*
161 Neurons were cultured on poly-D-lysine/laminin coated 6-well dishes and treated as described above.
162 Cells were collected by scraping into ice-cold PBS, pelleted, and immediately lysed in a small volume of
163 urea/CHAPS Lysis Buffer (9M urea, 2% CHAPS, in 30mM Tris, with 1x protease inhibitor cocktail
164 [Sigma]). Protein concentrations were determined by the Bradford method (Bradford, 1976; Hammond
165 and Kruger, 1988) and samples stored at -80°C until use. Samples were diluted in a reducing sample
166 buffer (Li-Cor) and boiled prior to use. Protein samples were then subjected to SDS-PAGE using Bio-Rad
167 pre-cast TGX gels and transferred to PVDF using a Bio-Rad SemiDry Transfer apparatus. Western blots
168 of the gels were then probed using rabbit anti-PGC1α (1:2000; Novus NBP1-04676), mouse anti-actin
169 (1:40,000, EMD Millipore MAB1501), mouse anti-COXIV (1:25,000; Abcam ab14744), and rabbit anti-

JNeurosci Accepted Manuscript

ATP5G1 (1:2,000; Abcam ab180149). Li-Cor Odyssey compatible IR680- and IR800-conjugated goat secondaries (Li-Cor) were used for detection, and blots were imaged and analyzed using a Li-Cor Odyssey Infrared Imaging System equipped with Odyssey Application Software Ver. 3.0.30.

Stimulated Emission Depletion (STED) Super-Resolution Imaging of Mitochondrial-ER Interaction

Primary cortical neurons were co-transfected with mtDsRed2 and GFP-Sec61β at DIV6. At DIV14, cells were treated with EdU (10μM) for 3hr, then fixed and fluorescently stained for EdU using the Click-iT Alexa Fluor 647 kit (ThermoFisher), and immunofluorescently stained for GFP using chicken anti-GFP (1:500; Abcam ab13970) and goat anti-chicken Alexa 488 (ThermoFisher). Stimulated emission depletion (STED) super-resolution microscopy was used to examine EdU staining relative to mitochondria and ER. STED microscopy was taken with a Leica TCS SP8 STED 3X system on Leica LAS X software. Image stacks were taken with 0.019 μm pixels and 0.100 μm z-steps using a 100x 1.4NA STED objective. A pulsed white light laser was used to excite the fluorophores, and emissions were collected using a filterless Acousto-Optical Beam Splitter (AOBS) system. DsRed2 was excited at 558nm and emissions collected from 563 to 648nm. Alexa 488 was excited at 496nm and emissions collected from 500 to 553 nm. Alexa 647 was excited at 653 and emissions collected from 658 to 767nm. A pulsed 775nm STED laser was used to achieve super-resolution. All emissions were temporally gated from 1.3 to 6 ns after the excitation pulse.

Experimental Design and Statistical Analysis

For data in Figures 2 and 3, primary cortical neurons from 3-6 separate, independent neuronal preparations (as indicated) were cultured on glass coverslips in individual wells of a 24-well dish or in individual microfluidic devices as described above. Neurons were cultured to DIV7, then individual

JNeurosci Accepted Manuscript

wells/devices were divided into 3 groups – Controls exposed only to DMSO vehicle and not to BrdU (*Control, no BrdU*), DMSO vehicle followed by BrdU treatment (*Control, +BrdU*), or 1nM rotenone followed by BrdU treatment (*Rotenone, +BrdU*). After treatments, cells were subjected to immunochemical staining and imaging as described above. Each individual field from the *Control, +BrdU* and *Rotenone, +BrdU* cells was thresholded to experiment-paired *Control, no BrdU* fields and quantified for BrdU puncta in cell bodies and outside cell bodies per field as described above. Data for the *Control, +BrdU* and *Rotenone, +BrdU* groups were compared and statistically analyzed by unpaired, two-tailed t test using GraphPad Prism analysis software (Ver 7.0c).

For data in Figures 4A-J, primary cortical neurons from 4 separate, independent neuronal preparations were cultured in 6-well culture dishes as described above. Neurons were cultured to DIV7, then wells divided into 2 groups – DMSO vehicle control and 1nM rotenone. Each condition was done in duplicate or triplicate on separate dishes, resulting in n=11-13 for each condition across 4 independent neuronal preparations. After 1wk or 2wk of treatments, cells were collected and subjected to Western blot and immunochemical detection analysis as described above. Data for the DMSO vehicle and 1nM rotenone groups were compared and statistically analyzed by unpaired, two-tailed t test using GraphPad Prism analysis software (Ver 7.0c). For COXIV intensity analysis (Figures 4K-N) primary cortical neurons from 3 separate, independent neuronal preparations (as indicated) were cultured in individual microfluidic devices as described above. Neurons were cultured to DIV7, then individual wells/devices were divided into 2 groups – Controls exposed to DMSO vehicle (*Control*), or 1nM rotenone (*Rotenone*). After 1 week of treatments, cells were subjected to immunochemical staining and imaging as described above. Each individual field from the axon chamber images and each individual cell from the cell chamber

JNeurosci Accepted Manuscript

images from the *Control* and *Rotenone* groups were quantified as described, and data compared and statistically analyzed by unpaired, two-tailed t test using GraphPad Prism analysis software (Ver 7.0c).

JNeurosci Accepted Manuscript

RESULTS

Detection of BrdU and EdU incorporation in primary neurons as a measure of mtDNA replication.

In order to assess specific anatomic localization of mitochondrial biogenesis within the neuron, we first optimized methodology to localize and quantify markers of biogenesis, via incorporation of the thymidine analog 5-bromo-2-deoxyuridine (BrdU) into mtDNA in cultured neurons as a measure of mtDNA replication (Amiri and Hollenbeck, 2008; Lentz et al., 2010). To establish mitochondrial BrdU detection in CNS neurons, we exposed primary cortical neurons at DIV14 to 10µM BrdU for various time points (15min-72hr), then fixed the cells. We then developed an immunocytochemical methodology that provided clear detection of BrdU-positive puncta in both cell bodies and neurites as described in *Methods*. We were able to detect mitochondrial BrdU incorporation within neurons as early as 15min (not shown), but consistent results were obtained at 1hr of incubation, similar to previous studies (Davis and Clayton, 1996). To verify mitochondrial localization, neurons were transfected at DIV6 to express mitochondrially-targeted photoactivatable GFP (PA-mtGFP), a mitochondrial marker that we found to be resistant to the acid treatment required in the BrdU immunochemical detection process. At DIV14, neurons were then treated with BrdU. At 1hr, BrdU incorporation was detected specifically in mitochondria both in soma and in distal axons (Figure 1A, D). As expected, BrdU puncta increased with prolonged (3hr) BrdU incubation (Figure 1B). Further, we did not observe BrdU in the nuclei of neurons, since they are post-mitotic cells. To further verify that BrdU puncta represented incorporation into mtDNA, we used 2',3'-dideoxycytidine (ddC), an inhibitor of mitochondrial polymerase gamma (Zimmermann et al., 1980; Starnes and Cheng, 1987), as a negative control. Co-treatment of 10µM BrdU with 100µM ddC prevented BrdU incorporation, even after 3hr of BrdU incubation (Figure 1C).

JNeurosci Accepted Manuscript

To further verify our findings with BrdU, we evaluated mtDNA replication using another thymidine analog, 5-ethynyl-2'-deoxyuridine (EdU), which can be detected via "click chemistry" reaction (Haines et al., 2010; Lentz et al., 2010), eliminating the acid denaturation required for immunochemical BrdU detection. Neurons expressing mitochondrially-targeted DsRed2 (mtDsRed) were exposed to 10µM EdU for 3hr. Similar to BrdU, we observed mitochondria-specific EdU puncta in both the soma and distal neurites of primary neurons (Figure 1E).

Chronic, sublethal rotenone exposure increases mtDNA replication rates first in neurites, and later in cell bodies.

As noted, we previously observed that mitochondrial density increased only in distal axons after 1wk exposure to chronic sublethal doses of rotenone (Arnold et al., 2011). After 2wk of chronic rotenone, we then observed increased mitochondrial density in both distal axons and cell bodies (Arnold et al., 2011). These data suggested the possibility of increased axon-specific mitochondrial biogenesis as an early response to chronic stress. To test this hypothesis, we examined whether chronic, low-dose rotenone exposure affected mtDNA replication in a similar neuroanatomic and temporal pattern. Beginning at DIV7, primary neurons were exposed to 1nM rotenone or DMSO vehicle control for 1wk or 2wk, a rotenone concentration we previously showed to result in minimal cell death (Arnold et al., 2011). Following rotenone treatment, neurons were pulsed for 1hr with 10µM BrdU, immunostained for BrdU and MAP2 (which in these cultures identify neuronal cell bodies, dendrites, and, weakly, axons), and evaluated by confocal analyses (Figure 2). To evaluate anatomical localization of BrdU puncta, image fields were processed to count puncta present specifically within cell bodies and outside cell bodies, as described in *Methods.*

JNeurosci Accepted Manuscript

Following 1wk of exposure to rotenone, we observed no change in mtDNA replication in the cell bodies at 1wk (Figure 2C). However, we observed a significant increase in the numbers of BrdU puncta detected in neurites of primary neurons (50±5 neurite puncta per field) as compared to vehicle-exposed control neurons (36±4 neuritic puncta per field, $p = 0.047$), a 1.4 fold increase (Figure 2D). After 2 wks of rotenone exposure, we then observed a significant increase in mtDNA replication rates in the soma (4.7±0.4 BrdU puncta per cell body) compared to vehicle-exposed control neurons (3.5±0.3 BrdU puncta per cell body, $p = 0.022$) (Figure 2G). Also, neuritic mtDNA replication remained significantly elevated at 2wk of rotenone exposure (53±4 neurite puncta per field) as compared to vehicle-exposed control neurons (42±3 neuritic puncta per field, $p = 0.023$) (Figure 2H). These data complement our previously observed early increase in axonal mitochondrial density after chronic rotenone exposure (Arnold et al., 2011). Of note, while incorporation of thymidine analogs occurs after DNA damage and repair, this is considered unlikely to contribute significantly to signal from these short BrdU incubations (Davis and Clayton, 1996). Further, we have shown previously that 10-fold higher doses of rotenone did not elicit any mtDNA damage in primary rat cortical neurons (Sanders et al., 2014).

mtDNA replication occurs specifically in distal axons, and rates are increased by low-level, chronic rotenone exposure.

The above results demonstrate that mitochondria with evidence of active mtDNA replication can be found in axons and dendrites, and also that rates of mtDNA replication increase in a compartmentalized manner following chronic rotenone exposure. Yet these studies cannot unequivocally confirm that the increased mtDNA replication is occurring specifically in distal axons, where we previously observed early rotenone-associated increases in mitochondrial density (Arnold et

JNeurosci Accepted Manuscript

al., 2011). Given the distribution of axons, dendrites and neuronal cell bodies across our cultures, it was not possible to identify distal axons conclusively. In addition, while we utilized the shortest BrdU incubation period possible in order to differentiate mtDNA replication in neurites from replication in cell bodies, we could not completely rule out an influence of axonal anterograde transport of newly-made mitochondria originating from the cell body. Thus, to answer definitively whether mtDNA replication, and therefore biogenesis, can occur specifically in distal axons, we utilized microfluidic devices in which we could isolate axons from cell bodies and dendrites, and could limit BrdU exposure to axonal mitochondria.

Neurons were cultured in microfluidic cell culturing devices with microchannels, environmentally separating cell bodies from their distal axon projections by 450µm or 900µm, allowing us to specifically evaluate distal axons (Figure 3A) (Taylor et al., 2005). We first confirmed that axons contain the transporter that imports nucleosides, including BrdU, the equilibrative nucleoside transporter (ENT-1) (Sivakumar et al., 2004). Immunocytochemistry revealed that primary cortical neuron distal axons do exhibit ENT-1 (Figure 3B). After verifying this, cell and axon chambers were treated for 1wk with 1nM rotenone or DMSO vehicle control as described above. At DIV14 (1wk of rotenone exposure), only the axon chamber of the microfluidic device was exposed to 10µM BrdU for 3hr. We then evaluated whether mtDNA replication could occur directly in distal axons. We indeed found mtDNA replication in the most distal axons, >500-1000µm from the channels (>1000-2000µm from their cell bodies; Figure 3C). Importantly, there was no BrdU incorporation observed on the cell body chamber side of the device after 3hr of incubation with BrdU in the axon chamber (Figure 3C). This eliminated the possibility that BrdU was diffusing from the axons to the cell bodies on the other side of the channel, becoming incorporated into replicating mtDNA in the cell body, and then being transported in those

JNeurosci Accepted Manuscript

mitochondria back to distal axons. In addition, co-treatment of the DNA polymerase inhibitor ddC exclusively in the axon chamber resulted in a significant decrease in detectable BrdU puncta (12±0.8 puncta/field after 3hr BrdU vs. 7±0.6 puncta/field after BrdU+ddC; n=48 [BrdU+ddc] and 73 [BrdU control] fields representing four independent neuron preps; difference in means = -4.6±1.1; $t(119) = 4.2$; $p = 0.000055$; two-tailed unpaired t-test). Thus, BrdU puncta present in the axons represent incorporation into mtDNA, originating there, rather than soma-based mitochondrial replication followed by transport.

We next examined the effect of rotenone specifically on distal axonal mtDNA replication. Both axon and cell body chambers were treated with 1nM rotenone for 1wk. We then exposed the axon chamber only to 10μM BrdU for 3hr. We found that 1wk treatment with rotenone significantly increased the rate of mtDNA replication (13.7±0.8 puncta per field) in distal axons as compared to vehicle-exposed control (9.8±0.6 puncta per field, $p = 0.0001$) (Figure 3D). This represents a 1.6 fold increase in mtDNA replication, corresponding with our previous results. This provided further proof that chronic exposure to low-dose, nonlethal concentrations of rotenone triggers direct, distal axonal mtDNA replication.

Changes in abundance of PGC1α, COXIV, and ATP5G1 in neurons follow different time course after chronic rotenone exposure.

To further assess mitochondrial biogenesis, we examined changes in levels of the mitochondrial biogenesis regulator and transcriptional co-activator, PGC1α, in cultured neurons (Figure 4). Protein lysates from neurons after 1wk of chronic rotenone exposure did not reveal any changes in PGC1α levels, but PGC1α abundance significantly increased after 2wk of rotenone exposure as compared to vehicle control (2wk rotenone PGC1α levels at 112% of control, $p = 0.0013$) (Figure 4C, H). This

JNeurosci Accepted Manuscript

suggests the possibility of distinct mechanisms for early axonal changes in biogenesis as compared to later cell body increases. To further evaluate this possibility, we examined levels of electron transport chain Cytochrome Oxidase subunit IV (COXIV). COXIV mRNA has been reported to be transported down distal axons and locally synthesized (Gioio et al., 2001; Aschrafi et al., 2016). We hypothesized that if local biogenesis was occurring in distal axons, we might see temporal asynchrony between PGC1α levels and upregulation of axonally translated mitochondrial protein levels. Specifically, we might expect rotenone exposure to lead to earlier increase in COXIV abundance (due to distal biogenesis) without a concomitant increase in PGC1α (acting at the nucleus later to upregulate transcription). Supporting this, we found that unlike PGC1α, COXIV levels were significantly increased following only 1wk of rotenone exposure as compared to vehicle control (1wk rotenone COXIV levels at 151% of control, $p = 0.020$), and remained significantly elevated after 2wk (2wk rotenone COXIV levels at 133% of control, $p = 0.044$) (Figure 4D, I). To add further support, we examined changes in levels of a second mitochondrial protein, ATP synthase subunit 9 (ATP5G1), a component of ETC Complex V. ATP5G1 mRNA has also been demonstrated to be transported down axons and locally translated there (Natera-Naranjo et al., 2012). Like COXIV levels, we found that ATP5G1 levels were also increased after 1 wk of chronic rotenone exposure (1wk rotenone ATP5G1 levels at 143% of control, $p = 0.028$), and remained elevated after 2 wks of exposure, relative to vehicle-treated control (2wk rotenone ATP5G1 levels at 123% of control, $p = 0.014$) (Figure 4E, J).

To further test the hypothesis that the early upregulated mitochondrial protein levels were indeed due to distal *axonal* mitochondrial biogenesis, we utilized the microfluidic chambers to separate immunochemical analysis of axons from cell bodies and dendrites, and evaluated anatomically localized COXIV levels after 1 wk of DMSO vehicle control or 1 nM rotenone exposure via

JNeurosci Accepted Manuscript

immunocytochemistry (Fig 4K, M). In axons, we found that COXIV protein levels were significantly increased following 1wk of 1nM rotenone as compared to vehicle control (1wk rotenone axonal COXIV levels at 132% of control, $p = 0.0005$) (Figure 4L). However, COXIV levels in the soma were not different between vehicle control and rotenone at 1wk (Figure 4N). These data suggest that the increase in whole-cell COXIV abundance we detected after 1wk of rotenone is largely due to the increase in COXIV protein levels specifically in the axons.

Evidence of mtDNA replication at mitochondrial-endoplasmic reticulum (ER) interaction sites within axons.

Mitochondrial replication and distribution to daughter mitochondria were recently reported to be initiated at mitochondrial-ER contact sites in replicating mammalian cells and yeast (Murley et al., 2013; Lewis et al., 2016). However, although ER has been demonstrated to extend throughout axonal networks in the CNS (Luarte et al., 2017), mtDNA replication at ER-mitochondrial contact sites in axons had never been demonstrated. We therefore examined the interaction of mitochondria and ER at sites of active mtDNA replication within axons. Primary cortical neurons were transfected to express mtDsRed2 and GFP-tagged ER protein Sec61beta (GFP-Sec61beta). After 1wk of expression, neurons were exposed to 10μM EdU for 3hr, fixed, and stained for both GFP and EdU. Using super-resolution stimulated emission depletion (STED) microscopy, we examined both soma and axons. We observed mitochondrial-ER interactions within the soma and neurites (Figure 5). In neurites, the mitochondria appeared to be nearly enveloped by ER (Figure 5B, C). Some mitochondria also displayed evidence of mtDNA replication via EdU incorporation. We observed mitochondria which exhibited EdU puncta at their tips (Figure 5B), which based on previous studies (Lewis et al., 2016) would suggest recently-

JNeurosci Accepted Manuscript

divided mitochondria, where division occurred at the site of mtDNA replication. We also observed mitochondria with EdU incorporation occurring at midpoints within their length, as opposed to the tips. At these points, ER showed intimate interaction with the mitochondria, wrapping around and overlapping the mtDNA replication site (Figure 5C). This is, to our knowledge, the first observation of mtDNA replication site interactions with ER in axons, providing further evidence of active biogenesis away from the cell body.

As further evidence that biogenesis likely takes place in axons, we performed immunocytochemistry for mitochondrial single-stranded DNA binding protein (mtSSBP), which binds specifically to single-stranded mtDNA during replication (Curth et al., 1994; Tiranti et al., 1995). After 3hr of BrdU exposure, we observed mtSSBP puncta co-localized to sites of BrdU incorporation within distal axonal mitochondria (Figure 5D).

DISCUSSION

In these studies, we provide evidence supporting the hypotheses that mitochondrial biogenesis occurs in distal CNS axons in addition to cell bodies, and that distal axonal mitochondrial biogenesis is upregulated in response to a chronic stressor linked to PD.

Mitochondrial biogenesis in distal axons.

It is generally assumed that mitochondrial biogenesis takes place only in cell bodies, in perinuclear regions, as has been shown for muscle cells and PC12 cells (Davis and Clayton, 1996; Schultz et al., 1998). However, our present studies demonstrated that mtDNA replication occurs in the most distal axons as well, providing new evidence that at least one important component of biogenesis of new

JNeurosci Accepted Manuscript

mitochondria does occur far from the cell body. In addition, we provided the first demonstration of mtDNA replication sites adjacent to ER in axons, providing evidence supporting localized axonal ER-mitochondrial sites of replication and division into new mitochondria, as was previously observed in cell bodies of yeast and replicating mammalian cells (Murley et al., 2013; Lewis et al., 2016). Although it is difficult to definitively delineate neuroanatomical localization of mitochondrial biogenesis, since most other measures of biogenesis cannot give anatomical localization, our present findings are bolstered by our previously reported findings of increased mitochondrial density in neurons under similar conditions (Arnold et al., 2011). In that study, under similar chronic exposures, we found localized increases in mitochondrial density in distal axons — without evidence of increased anterograde transport, decreased retrograde transport, decreased distal mitophagy, or concurrent mitochondrial density increases in the soma —further supporting the presence of axonal biogenesis.

Coordination of the components of mitochondrial biogenesis in neurons is not well understood. The supposition that mitochondrial biogenesis takes place only in neuronal cell bodies, near nuclei, with new mitochondria transported to distal regions via axonal transport, arises from the fact that translation of nuclear-encoded, mitochondrially-targeted proteins has to be coordinated with membrane biosynthesis, mtDNA replication, and mitochondrial division (Davis and Clayton, 1996; Nisoli et al., 2004). In addition, upregulation of nuclear gene expression for mitochondrially-targeted proteins and mitochondrial transcription factors via the nuclear transcription co-activator PGC1α is one known regulator of the coordinated mitochondrial biogenesis process (Stevens et al., 2015; Lee et al., 2017). However, a system that would not allow for biogenesis locally would be an inefficient means of replacing dysfunctional mitochondria at distal terminals of long axons, and thus would seem detrimental to survival in neurons with long or high-energy-demand projections. This is particularly

JNeurosci Accepted Manuscript

425 relevant to neuronal populations vulnerable in PD neurodegeneration, which contain particularly long
426 axons with extensive arborization (Braak et al., 2004; Surmeier et al., 2017).
427
428 The present study is the first to examine mitochondrial biogenesis directly in CNS distal axons. There
429 has been previous support for non-cell body mtDNA replication in the peripheral nervous system
430 (PNS). Two studies using thymidine analogs in PNS neurons detected mtDNA replication in both soma
431 and proximal neurites (Amiri and Hollenbeck, 2008; Lentz et al., 2010), with one study showing that
432 mtDNA replication occurred in the axons of peripheral sympathetic ganglia neurons after being
433 physically separated from cell bodies (Amiri and Hollenbeck, 2008). A third study was performed in CNS
434 neurons, examining BrdU incorporation into both somal and neuritic mitochondria in mouse
435 hippocampal neurons after acute exposure to toxicants and in neurons from a transgenic mouse
436 Alzheimer disease model (Calkins and Reddy, 2011). However, neuritic origin of the mtDNA replication
437 could not be distinguished from transported somal mitochondria in that study, since prolonged BrdU
438 exposure periods (20 hours) were utilized, and distal axons were not delineated. Our present studies,
439 then, provide the first definitive confirmation of CNS distal axonal mtDNA replication, and further link
440 it to both increased mitochondrial density and mitochondrial-ER localization.
441
442 *Exposure to a chronic PD-relevant stressor may cause early increased axonal mitochondrial biogenesis.*
443 Chronic exposure to low, non-lethal concentrations of the mitochondrial toxin rotenone results in a
444 specific PD phenotype in rats, with neurodegeneration and pathological changes typical of human
445 disease (Betarbet et al., 2000; Cannon et al., 2009), and chronic rotenone is an established PD model.
446 Rotenone exposure is a risk factor in human PD (Tanner et al., 2011; Wirdefeldt et al., 2011), and
447 elucidation of mechanisms involved in chronic rotenone exposure is likely to yield information relevant

JNeurosci Accepted Manuscript

448 to PD neuropathogenesis. Both human PD and chronic rotenone exposure lead to loss of dopaminergic
449 axon loss first, then followed by cell death (Betarbet et al., 2000; Tagliaferro and Burke, 2016).
450 Therefore, early adverse effects on distal axonal mitochondrial homeostasis may have key involvement
451 in initial changes leading to later neuron death.
452
453 We previously demonstrated that low-dose rotenone exposure results in early changes in axonal
454 mitochondrial fission, fusion, and transport prior to cell death (Arnold et al., 2011). We also observed a
455 temporal effect of increasing mitochondrial density, where mitochondrial density in distal axons
456 increased early and without concurrent increases in somal density, but density was increased in both
457 axons and cell bodies at later time points (Arnold et al., 2011). Our present studies demonstrate similar
458 time-dependent alterations in distal axonal mtDNA replication after chronic exposure to
459 concentrations of rotenone that cause early neurite pathology but no cell death. Initially, chronic
460 sublethal rotenone exposure caused increased mtDNA replication localized to neurites, and only after
461 longer exposures is there a concomitant increase in cell body mtDNA replication. Our work further
462 confirms that chronic rotenone exposure increases mtDNA replication specifically in distal axons, along
463 with concomitant upregulation of mitochondrially-targeted protein known to be locally translated in
464 axons via axonally transported mRNA. These changes correlate to the anatomic localization and time
465 course of increases in mitochondrial density in neurons after rotenone exposure observed in our
466 previous work (Arnold et al., 2011).
467
468 We hypothesize that the rotenone-induced early upregulation mitochondrial biogenesis in axons, and
469 increased mitochondrial density, is a compensatory process in response to chronic low-level
470 mitochondrial disruption, in an attempt to prevent cell death. In neurons with a lower capacity for

JNeurosci Accepted Manuscript

axonal mitochondrial biogenesis, risk for subsequent neuron death would be increased. If the localized mitochondrial biogenesis response is insufficient, mitochondrial stress in energy-requiring distal axons could trigger axonal neurodegeneration and subsequent neuronal cell death. This is particularly relevant for PD neurodegeneration, since it is known that genes such as Parkin, whose loss-of-function mutations cause PD, are known to regulate mitochondrial biogenesis (Stevens et al., 2015; Lee et al., 2017).

Proposed model of early and late regulation of neuronal mitochondrial biogenesis in response to PD-relevant chronic stress.

Our present studies support the following proposed model: After initiation of a chronic neurotoxic exposure such as rotenone, known to result in axonal loss prior to cell death, the initial response to mitochondrial stress may be upregulation of biogenesis through *localized* means (Figure 7). Detailed imaging studies have demonstrated that ribosomes on ER, capable of protein translation, are present throughout the length of axons (Luarte et al., 2017). mRNAs of nuclear-expressed mitochondrially-targeted proteins have been shown to be transported down axons, and regulation of axon protein expression affects mitochondrial function (Gioio et al., 2001; Hillefors et al., 2007; Willis et al., 2011; Spillane et al., 2013; Minis et al., 2014; Aschrafi et al., 2016). More directly, dynamic regulation of localized translation of nuclear-expressed mitochondrially-targeted proteins in axons has been recently demonstrated (Shigeoka et al., 2018). We believe it is possible that in distal axons, a localized pool of mRNA and translation machinery, combined with signaling mechanisms for mtDNA replication and other steps of biogenesis, are available for more rapid upregulation of mitochondrially-targeted protein synthesis, particularly in response to stress. As stress continues over a longer period, PGC1α is upregulated, leading to transcriptional co-activation of downstream effectors which could then

JNeurosci Accepted Manuscript

upregulate overall mitochondrial biogenesis throughout the neuron. An inadequate early compensatory response to stress in the axons of vulnerable neurons, then, could lead to initiation of neurodegeneration. Further studies are necessary to verify this hypothesized model.

REFERENCES

Amiri M, Hollenbeck PJ (2008) Mitochondrial biogenesis in the axons of vertebrate peripheral neurons. Dev Neurobiol 68:1348-1361.

Arnold B, Cassady SJ, VanLaar VS, Berman SB (2011) Integrating multiple aspects of mitochondrial dynamics in neurons: age-related differences and dynamic changes in a chronic rotenone model. Neurobiol Dis 41:189-200.

Aschrafi A, Kar AN, Gale JR, Elkahloun AG, Vargas JN, Sales N, Wilson G, Tompkins M, Gioio AE, Kaplan BB (2016) A heterogeneous population of nuclear-encoded mitochondrial mRNAs is present in the axons of primary sympathetic neurons. Mitochondrion 30:18-23.

Betarbet R, Sherer TB, MacKenzie G, Garcia-Osuna M, Panov AV, Greenamyre JT (2000) Chronic systemic pesticide exposure reproduces features of Parkinson's disease. Nat Neurosci 3:1301-1306.

Berman SB, Chen YB, Qi B, McCaffery JM, Rucker EB 3rd, Goebbels S, Nave KA, Arnold BA, Jonas EA, Pineda FJ, Hardwick JM (2009) Bcl-x L increases mitochondrial fission, fusion, and biomass in neurons. J Cell Biol 184(5):707-719.

Bose A, Beal MF (2016) Mitochondrial dysfunction in Parkinson's disease. J Neurochem 139 Suppl 1:216-231.

Braak H, Ghebremedhin E, Rub U, Bratzke H, Del Tredici K (2004) Stages in the development of Parkinson's disease-related pathology. Cell Tissue Res 318:121-134.

Bradford MM (1976) A rapid and sensitive method for the quantitation of microgram quantities of protein utilizing the principle of protein-dye binding. Anal Biochem 72:248-254.

Calkins MJ, Reddy PH (2011) Assessment of newly synthesized mitochondrial DNA using BrdU labeling in primary neurons from Alzheimer's disease mice: Implications for impaired mitochondrial biogenesis and synaptic damage. Biochim Biophys Acta.

Cannon JR, Tapias V, Na HM, Honick AS, Drolet RE, Greenamyre JT (2009) A highly reproducible rotenone model of Parkinson's disease. Neurobiol Dis 34:279-290.

Curth U, Urbanke C, Greipel J, Gerberding H, Tiranti V, Zeviani M (1994) Single-stranded-DNA-binding proteins from human mitochondria and Escherichia coli have analogous physicochemical properties. Eur J Biochem 221:435-443.

Davis AF, Clayton DA (1996) In situ localization of mitochondrial DNA replication in intact mammalian cells. J Cell Biol 135:883-893.

Detmer SA, Chan DC (2007) Functions and dysfunctions of mitochondrial dynamics. Nat Rev Mol Cell Biol 8:870-879.

Gioio AE, Eyman M, Zhang H, Lavina ZS, Giuditta A, Kaplan BB (2001) Local synthesis of nuclear-encoded mitochondrial proteins in the presynaptic nerve terminal. J Neurosci Res 64:447-453.

Haines KM, Feldman EL, Lentz SI (2010) Visualization of mitochondrial DNA replication in individual cells by EdU signal amplification. J Vis Exp.

Hammond JB, Kruger NJ (1988) The bradford method for protein quantitation. Methods Mol Biol 3:25-32.

JNeurosci Accepted Manuscript

536 Hillefors M, Gioio AE, Mameza MG, Kaplan BB (2007) Axon viability and mitochondrial function are
537 dependent on local protein synthesis in sympathetic neurons. Cell Mol Neurobiol 27:701-716.
538 Kar AN, Sun CY, Reichard K, Gervasi NM, Pickel J, Nakazawa K, Gioio AE, Kaplan BB (2014) Dysregulation
539 of the axonal trafficking of nuclear-encoded mitochondrial mRNA alters neuronal mitochondrial
540 activity and mouse behavior. Dev Neurobiol 74:333-350.
541 Karbowski M, Arnoult D, Chen H, Chan DC, Smith CL, Youle RJ (2004) Quantitation of mitochondrial
542 dynamics by photolabeling of individual organelles shows that mitochondrial fusion is blocked
543 during the Bax activation phase of apoptosis. J Cell Biol 164:493-499.
544 Lee Y et al. (2017) PINK1 Primes Parkin-Mediated Ubiquitination of PARIS in Dopaminergic Neuronal
545 Survival. Cell Rep 18:918-932.
546 Lentz SI, Edwards JL, Backus C, McLean LL, Haines KM, Feldman EL (2010) Mitochondrial DNA (mtDNA)
547 biogenesis: visualization and duel incorporation of BrdU and EdU into newly synthesized
548 mtDNA in vitro. J Histochem Cytochem 58:207-218.
549 Lewis SC, Uchiyama LF, Nunnari J (2016) ER-mitochondria contacts couple mtDNA synthesis with
550 mitochondrial division in human cells. Science 353:aaf5549.
551 Li PA, Hou X, Hao S (2017) Mitochondrial biogenesis in neurodegeneration. J Neurosci Res 95:2025-
552 2029.
553 Luarte A, Cornejo VH, Bertin F, Gallardo J, Couve A (2017) The axonal endoplasmic reticulum: One
554 organelle-many functions in development, maintenance, and plasticity. Dev Neurobiol.
555 McCoy MK, Cookson MR (2012) Mitochondrial quality control and dynamics in Parkinson's disease.
556 Antioxid Redox Signal 16:869-882.
557 Minis A, Dahary D, Manor O, Leshkowitz D, Pilpel Y, Yaron A (2014) Subcellular transcriptomics-
558 dissection of the mRNA composition in the axonal compartment of sensory neurons. Dev
559 Neurobiol 74:365-381.
560 Murley A, Lackner LL, Osman C, West M, Voeltz GK, Walter P, Nunnari J (2013) ER-associated
561 mitochondrial division links the distribution of mitochondria and mitochondrial DNA in yeast.
562 Elife 2:e00422.
563 Natera-Naranjo O, Kar AN, Aschrafi A, Gervasi NM, Macgibeny MA, Gioio AE, Kaplan BB (2012) Local
564 translation of ATP synthase subunit 9 mRNA alters ATP levels and the production of ROS in the
565 axon. Mol Cell Neurosci. 49(3):263-270.
566 Nisoli E, Clementi E, Moncada S, Carruba MO (2004) Mitochondrial biogenesis as a cellular signaling
567 framework. Biochem Pharmacol 67:1-15.
568 O'Donnell KC, Lulla A, Stahl MC, Wheat ND, Bronstein JM, Sagasti A (2014) Axon degeneration and
569 PGC-1alpha-mediated protection in a zebrafish model of alpha-synuclein toxicity. Dis Model
570 Mech 7:571-582.
571 Sanders LH, McCoy J, Hu X, Mastroberardino PG, Dickinson BC, Chang CJ, Chu CT, Van Houten B,
572 Greenamyre JT (2014) Mitochondrial DNA damage: molecular marker of vulnerable nigral
573 neurons in Parkinson's disease. Neurobiol Dis 70:214-223.
574 Schindelin J, Arganda-Carreras I, Frise E, Kaynig V, Longair M, Pietzsch T, Preibisch S, Rueden C, Saalfeld
575 S, Schmid B, Tinevez JY, White DJ, Hartenstein V, Eliceiri K, Tomancak P, Cardona A (2012) Fiji:
576 an open-source platform for biological-image analysis. Nature methods 9:676-682.
577 Schneider CA, Rasband WS, Eliceiri KW (2012) NIH Image to ImageJ: 25 years of image analysis. Nature
578 methods 9:671-675.
579 Schultz RA, Swoap SJ, McDaniel LD, Zhang B, Koon EC, Garry DJ, Li K, Williams RS (1998) Differential
580 expression of mitochondrial DNA replication factors in mammalian tissues. J Biol Chem
581 273:3447-3451.

JNeurosci Accepted Manuscript

582 Shigeoka T, Jung J, Holt CE, Jung H (2018) Axon-TRAP-RiboTag: Affinity Purification of Translated
583 mRNAs from Neuronal Axons in Mouse In Vivo. Methods Mol Biol 1649:85-94.
584 Sivakumar S, Porter-Goff M, Patel PK, Benoit K, Rhind N (2004) In vivo labeling of fission yeast DNA
585 with thymidine and thymidine analogs. Methods 33:213-219.
586 Spillane M, Ketschek A, Merianda TT, Twiss JL, Gallo G (2013) Mitochondria coordinate sites of axon
587 branching through localized intra-axonal protein synthesis. Cell Rep 5:1564-1575.
588 Starnes MC, Cheng YC (1987) Cellular metabolism of 2',3'-dideoxycytidine, a compound active against
589 human immunodeficiency virus in vitro. J Biol Chem 262:988-991.
590 Stevens DA, Lee Y, Kang HC, Lee BD, Lee YI, Bower A, Jiang H, Kang SU, Andrabi SA, Dawson VL, Shin JH,
591 Dawson TM (2015) Parkin loss leads to PARIS-dependent declines in mitochondrial mass and
592 respiration. Proc Natl Acad Sci U S A 112:11696-11701.
593 Surmeier DJ, Obeso JA, Halliday GM (2017) Selective neuronal vulnerability in Parkinson disease. Nat
594 Rev Neurosci 18:101-113.
595 Tagliaferro P, Burke RE (2016) Retrograde Axonal Degeneration in Parkinson Disease. J Parkinsons Dis
596 6:1-15.
597 Tanner CM, Kamel F, Ross GW, Hoppin JA, Goldman SM, Korell M, Marras C, Bhudhikanok GS, Kasten
598 M, Chade AR, Comyns K, Richards MB, Meng C, Priestley B, Fernandez HH, Cambi F, Umbach
599 DM, Blair A, Sandler DP, Langston JW (2011) Rotenone, paraquat, and Parkinson's disease.
600 Environmental health perspectives 119:866-872.
601 Taylor AM, Blurton-Jones M, Rhee SW, Cribbs DH, Cotman CW, Jeon NL (2005) A microfluidic culture
602 platform for CNS axonal injury, regeneration and transport. Nat Methods 2:599-605.
603 Tiranti V, Rossi E, Ruiz-Carrillo A, Rossi G, Rocchi M, DiDonato S, Zuffardi O, Zeviani M (1995)
604 Chromosomal localization of mitochondrial transcription factor A (TCF6), single-stranded DNA-
605 binding protein (SSBP), and endonuclease G (ENDOG), three human housekeeping genes
606 involved in mitochondrial biogenesis. Genomics 25:559-564.
607 Van Laar VS, Berman SB (2009) Mitochondrial dynamics in Parkinson's disease. Exp Neurol 218:247-
608 256.
609 Van Laar VS, Berman SB (2013) The interplay of neuronal mitochondrial dynamics and bioenergetics:
610 implications for Parkinson's disease. Neurobiol Dis 51:43-55.
611 Voeltz GK, Prinz WA, Shibata Y, Rist JM, Rapoport TA (2006) A class of membrane proteins shaping the
612 tubular endoplasmic reticulum. Cell 124:573-586.
613 Willis DE, Xu M, Donnelly CJ, Tep C, Kendall M, Erenstheyn M, English AW, Schanen NC, Kirn-Safran CB,
614 Yoon SO, Bassell GJ, Twiss JL (2011) Axonal Localization of transgene mRNA in mature PNS and
615 CNS neurons. J Neurosci 31:14481-14487.
616 Wirdefeldt K, Adami HO, Cole P, Trichopoulos D, Mandel J (2011) Epidemiology and etiology of
617 Parkinson's disease: a review of the evidence. Eur J Epidemiol 26 Suppl 1:S1-58.
618 Zimmermann W, Chen SM, Bolden A, Weissbach A (1980) Mitochondrial DNA replication does not
619 involve DNA polymerase alpha. J Biol Chem 255:11847-11852.

JNeurosci Accepted Manuscript

FIGURE LEGENDS

Figure 1

Incorporation of BrdU and EdU into neuronal mitochondria in cell bodies and axons within 1-3hr of exposure.

A-C) Primary neurons (DIV14) expressing mitochondrially-targeted photoactivatible GFP (Mitochondria) were treated with 10μM BrdU for 1hr (A) or 3hr (B). Control cells were incubated with 100μM dideoxycytidine (ddC), an inhibitor of mitochondrial DNA polymerase gamma, for 6hr prior to and then during 3hr of BrdU exposure (C). Cells were immunofluorescently stained for BrdU, and confocal imaging revealed BrdU puncta associated with mitochondria in cell bodies (A, B), but minimal, if any, incorporation when ddC was present (C), confirming specificity for mtDNA replication. D) BrdU puncta were also found in mitochondria of distal axons after 1hr of BrdU exposure. E) Primary neurons (DIV14) expressing mitochondrially-targeted DsRed2 (Mitochondria) were treated with EdU for 3hr, then stained using the EdU Click-iT system. EdU positive puncta were again observed in mitochondria of the cell body and axons (E; *arrow*).

Figure 2

Quantifying localized mtDNA replication in soma and neurites of primary neurons in response to chronic exposure to rotenone.

A-B) Representative confocal z-stack images of neurons exposed to 10μM BrdU for 1hr following exposure to 1wk of DMSO vehicle control (A) or 1nM rotenone (B). C) Quantitative analysis of BrdU puncta revealed no difference in number of puncta per cell body between control and rotenone at 1wk ($t(78) = 0.012$; $p = 0.99$; two-tailed unpaired t-test; puncta/cell body ± SEM). D) In neurites, we observed a significantly increased number of BrdU puncta of rotenone-exposed neurons compared to vehicle control at 1wk (difference in means = +13.2; $t(78)= 2.02$; *$p = 0.047$; two-tailed unpaired t-test; puncta in processes/field ± SEM). (n=38 [control] and 42 [rotenone] image fields representing three independent neuronal preps)

E-F) Representative confocal z-stack images of neurons exposed to 10μM BrdU for 1hr following exposure to 2wk of DMSO vehicle control (E) or 1nM rotenone (F). G-H) Quantitative analysis of BrdU puncta revealed significant rotenone-associated increases in both cell bodies (G; difference in means =

JNeurosci Accepted Manuscript

+1.2; t(81) = 2.34; *p = 0.022; two-tailed unpaired t-test; puncta/cell body ± SEM) and neurites (H; difference in means = +11.3; t(81) = 2.32; *p = 0.023; two-tailed unpaired t-test; puncta in processes/field± SEM) compared to vehicle control at 2wk. (*n*=40 [control] and 43 [rotenone] image fields representing three independent neuron preps; ± SEM)

Figure 3

Distal axonal mtDNA replication is increased in response to chronic rotenone.

A) Primary neurons were seeded into one side of microfluidic devices (Xona microfluidics) in order to environmentally separate cell bodies and dendrites from axons for BrdU incorporation assessments. B) Neurons were transfected to express mitochondrially-targeted mtDsRed2 (Mitochondria), and at DIV14 were immunofluorescently stained to detect equilibrative nucleoside transporter 1 (ENT-1), to ensure that axons were capable of importing BrdU on their own (TLI: transmitted light image). C) Following 1wk of DMSO vehicle *(shown)* or 1nM rotenone, only the axons were exposed to 10µM BrdU for 3hr. Confocal imaging of immunofluorescence for BrdU incorporation show that axon-localized BrdU puncta can be found distally from the microfluidic grooves *(arrows)*, with no BrdU incorporation on the cell chamber side of the device. This suggests that mtDNA replication does occur locally in distal axons. D) Quantification of BrdU puncta demonstrated that mtDNA replication in distal axons was significantly increased following 1wk of chronic 1nM rotenone exposure, as compared to DMSO vehicle control. (*n*=123 image fields per condition representing six independent neuron preps; difference in means = +3.9; t(244) = 4; *p = 0.0001; two-tailed unpaired t-test; puncta in processes/field ± SEM)

Figure 4

Effect of chronic rotenone on neuronal expression of PGC1α and COXIV.

Primary neurons were treated with DMSO vehicle control or 1nM rotenone for 1wk (A-E) or 2wk (F-J), and collected for Western blot and immunochemical detection analyses of PGC1α and COXIV (A, F), and of ATP5G1 (B, G). C) We observed that 1wk of chronic rotenone exposure did not alter PGC1α levels (t(21) = 0.17; p = 0.87; two-tailed unpaired t-test). D) Levels of COXIV were significantly increased after 1wk of rotenone exposure as compared to vehicle control (difference in means = +51.4; t(21) = 2.5; *p = 0.020; two-tailed unpaired t-test). E) Levels of ATP5G1 were also significantly increased after 1wk of rotenone exposure as compared to vehicle control difference in means = +43.2; t(24) = 2.3; *p = 0.028; two-tailed unpaired t-test). H) After 2wk of chronic rotenone exposure, PGC1α levels were significantly increased as compared to vehicle control (difference in means = +11.7; t(22) = 3.7; *p = 0.0013; two-tailed unpaired t-test). I) Levels of COXIV remained significantly elevated after 2wk of rotenone exposure as compared to vehicle control (difference in means = +33.2; t(22) = 2.14; p =

JNeurosci Accepted Manuscript

693 0.044; two-tailed unpaired t-test). J) Levels of ATP5G1 also remained significantly increased after 2wk
694 of rotenone exposure as compared to vehicle control (difference in means = +23.3; t(24) = 2.66; p =
695 0.014; two-tailed unpaired t-test). (*n*=11-13; percent of control ± SEM)
696
697 To assess neuroanatomical localization of changes in COXIV protein, primary neurons were grown in
698 microfluidic devices (Xona microfluidics) in order to environmentally separate cell bodies and dendrites
699 from axons. K, M) Neurons were treated with DMSO vehicle control or 1nM rotenone for 1wk, then
700 fixed for fluorescent immunochemical detection of COXIV and detection of actin via phalloidin. L)
701 Quantitative fluorescence analyses demonstrated that after 1wk of 1nM rotenone, COXIV protein
702 levels in axons significantly increased as compared to vehicle control control (difference in
703 means=+31.8; t(47) = 3.72; p = 0.0005; two-tailed unpaired t-test) (*n*=26 [control] and 23 [rotenone]
704 image fields representing three independent neuron preps; ± SEM). N) COXIV levels in cell bodies,
705 however, were unchanged following 1wk of rotenone as compared to control (t(151) = 0.17; p = 0.87;
706 two-tailed unpaired t-test) (*n*=91 [control] and 62 [rotenone] cells representing three independent
707 neuron preps; ± SEM).
708
709
710
711 **Figure 5**
712
713 **Stimulated emission depletion (STED) super-resolution microscopy reveals mitochondrial-ER**
714 **interaction at axonal mtDNA replication sites, and mtSSBP localization suggests active mtDNA**
715 **replication in axons.**
716 A-C) Primary cortical neurons were co-transfected with mtDsRed2 (Mitochondria, Mitochondrion) and
717 GFP-tagged endoplasmic reticulum protein Sec61β (ER). At DIV14, cells were exposed to EdU (10μM)
718 for 3hr, then fixed and stained for EdU using the Click-iT Alexa Fluor 647 kit and for GFP via
719 immunofluorescence. STED super-resolution microscopy was used to examine EdU staining relative to
720 both mitochondria and ER in the soma (A) and in axons (B,C). We observed mitochondria-ER
721 interaction in axons (B; *green arrowheads*) and specifically at sites of mtDNA EdU incorporation (C;
722 *white arrow*). D) Primary neurons were transfected with PA-mtGFP (Mitochondria), and at DIV14
723 exposed to BrdU (10μM) for 3hr. Cells were immunofluorescently stained for BrdU and mitochondrial
724 single-stranded DNA binding protein (mtSSBP). We observed mtSSBP co-localized with BrdU puncta
725 within distal axonal mitochondria, suggesting active mtDNA replication.
726
727
728 **Figure 6**
729
730 **Proposed model of compartmentalized mitochondrial biogenesis response to stress in neurons**
731 ***Early Response to Chronic Stress***: As an initial response to low, chronic mitochondrial stress, high-
732 energy demanding arborized distal axons upregulate mitochondrial biogenesis locally, increasing

JNeurosci Accepted Manuscript

733 mtDNA replication, mRNA translation, and mitochondrial density in order to preserve axonal health
734 and function. This happens independent of the soma, where no significant changes in mitochondrial
735 biogenesis have yet occurred.
736 ***Later Response to Chronic Stress:*** As prolonged stress continues to tax mitochondrial function, nuclear
737 upregulation of the 'master mitochondrial biogenesis regulator', transcription co-activator PGC1α,
738 increases activation of mitochondrial biogenesis transcription factors (TFs), including NRF-1 and -2.
739 Mitochondrial biogenesis increases in the soma, leading to increased somal mitochondrial density, and
740 increased resources (such as nuclear-expressed mitochondrially-targeted transcription factors,
741 proteins, and mRNAs) are available for transport down the axon to maintain localized mitochondrial
742 biogenesis distally.
743 ***Pathogenic Conditions in Vulnerable Neurons:*** Neurons vulnerable to mitochondrial stressors may
744 lack the ability to quickly upregulate local mitochondrial biogenesis in distal axons in response to
745 stress. The poor early response to mitochondrial distress in the distal axon may lead to loss of the
746 axonal projection, and subsequent death of the neuron.
747

JNeurosci Accepted Manuscript

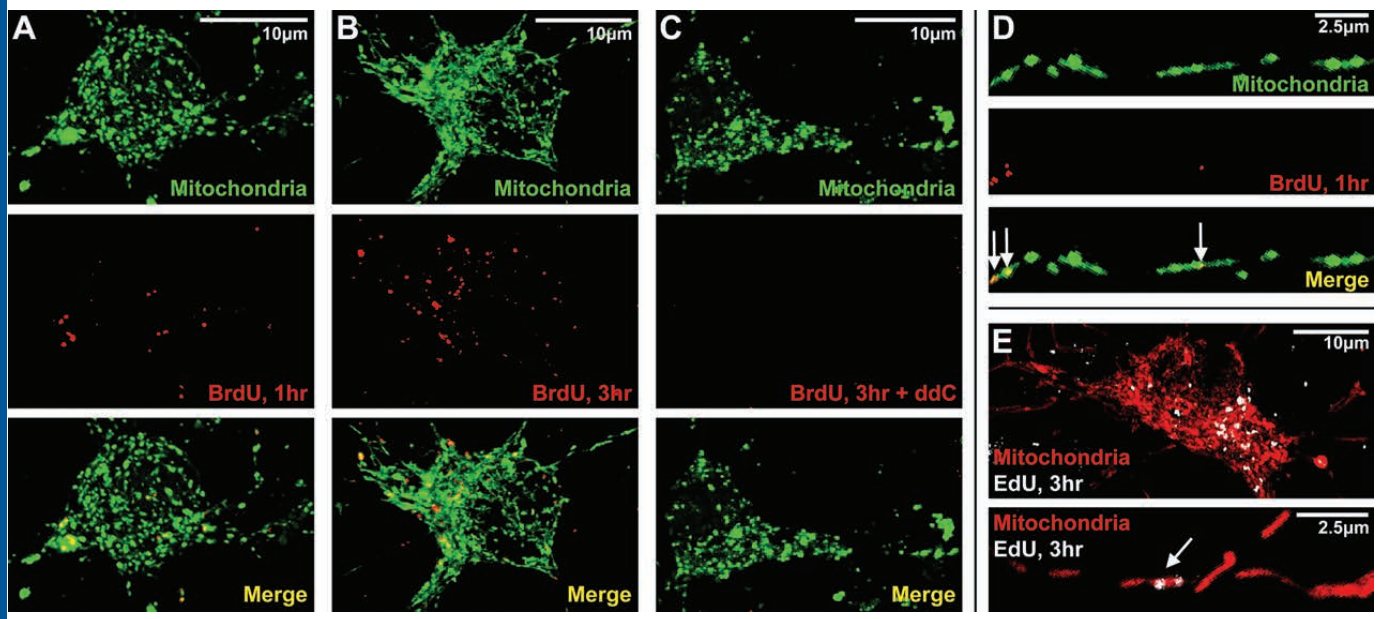

JNeurosci Accepted Manuscript

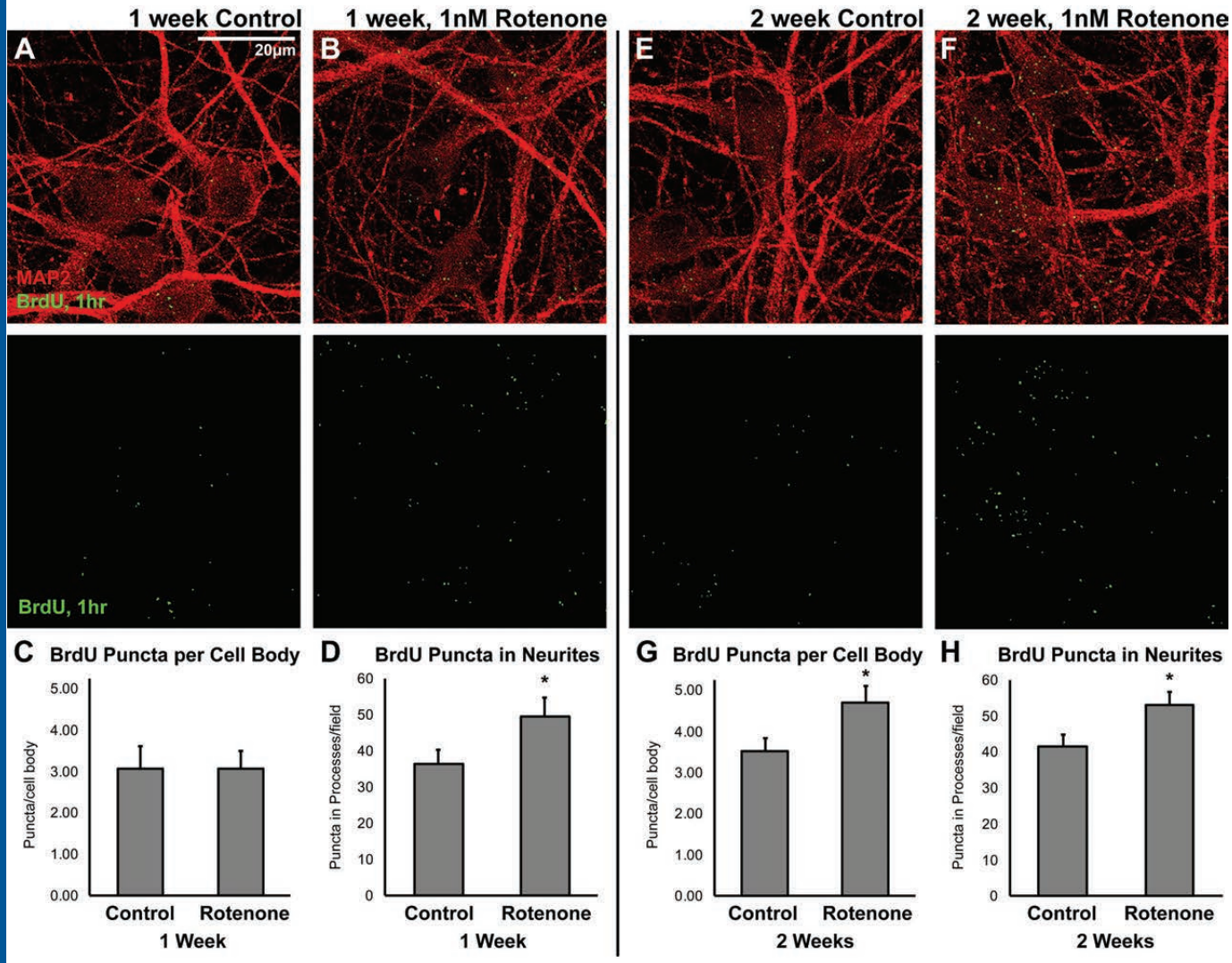

JNeurosci Accepted Manuscript

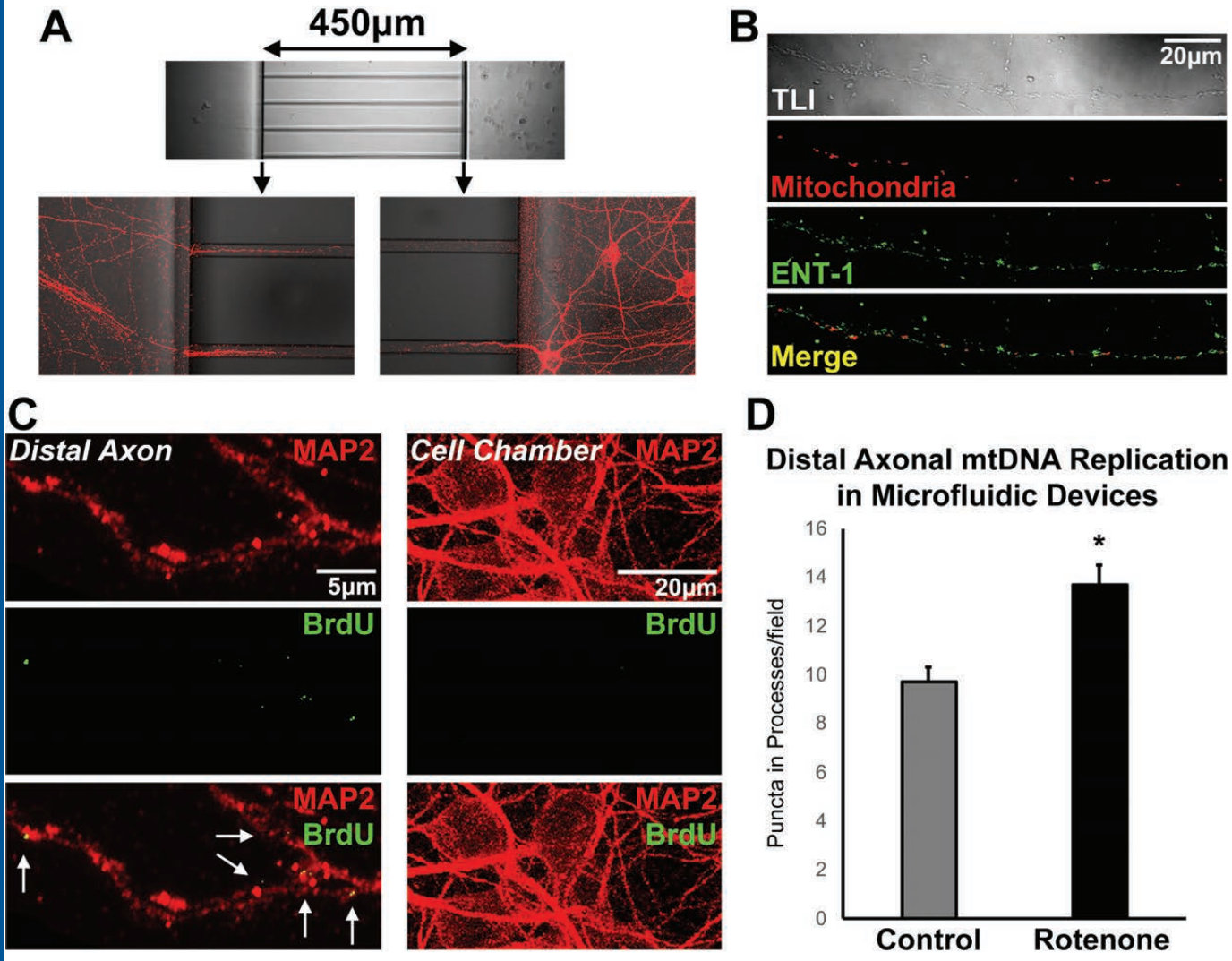

JNeurosci Accepted Manuscript

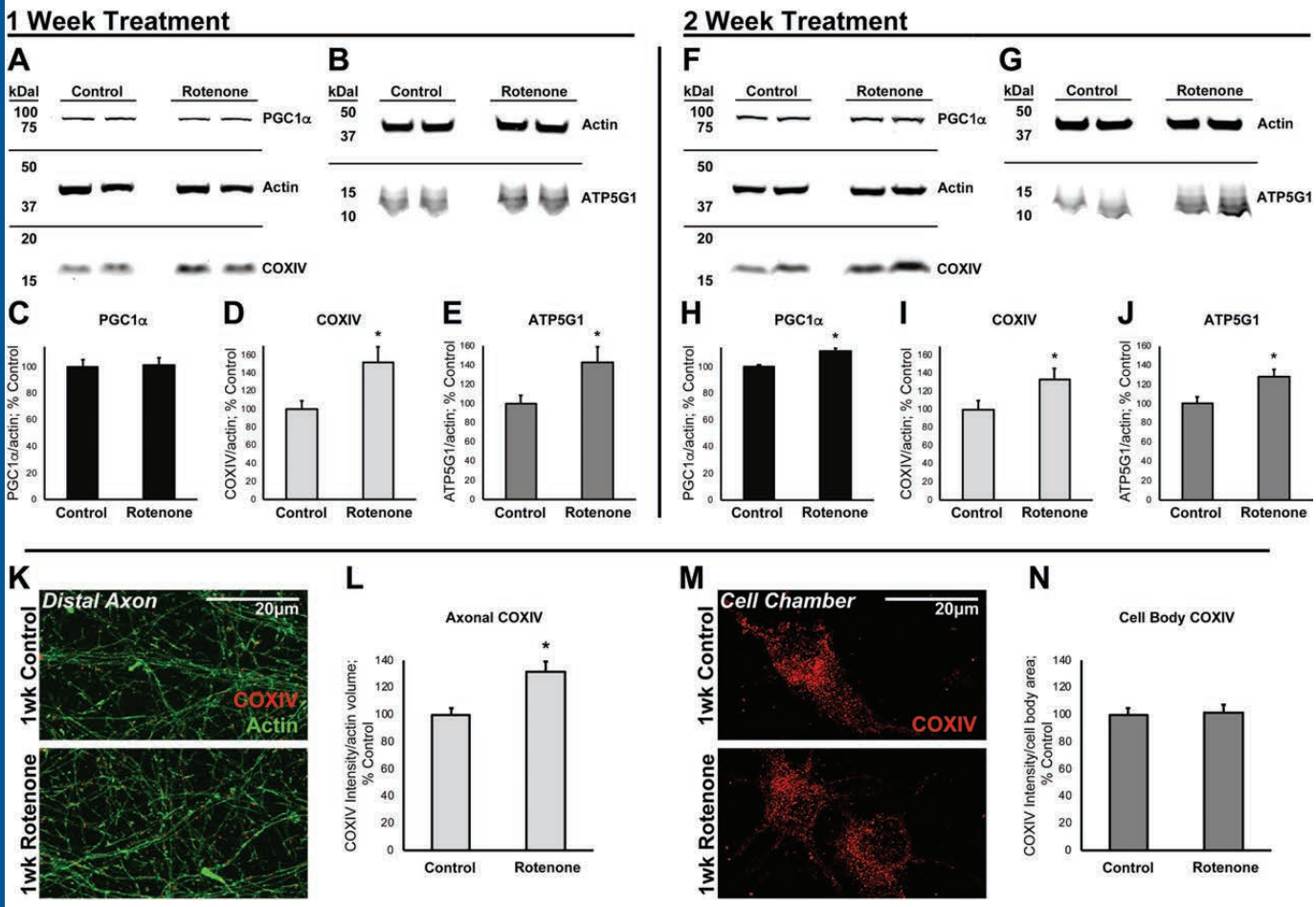

JNeurosci Accepted Manuscript

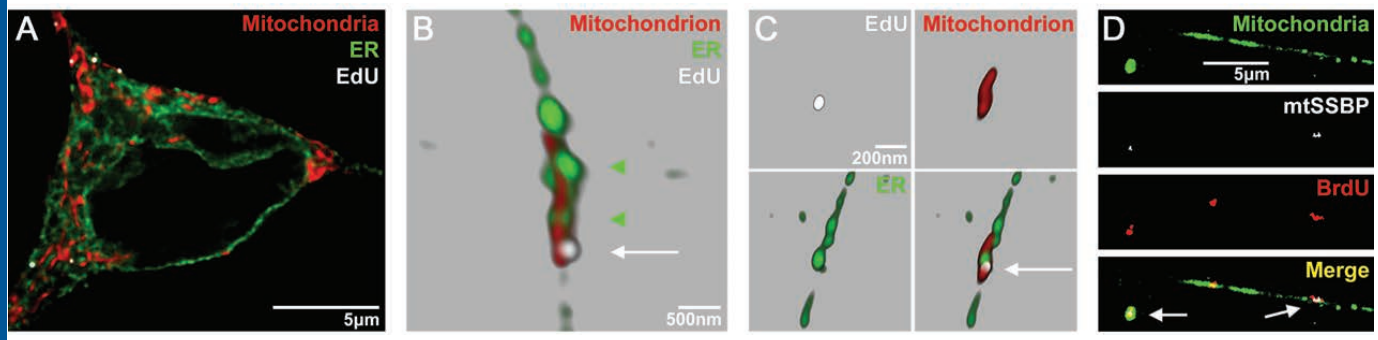

JNeurosci Accepted Manuscript

Early Response to Chronic Stress

Soma: No significant changes in mitochondrial biogenesis early

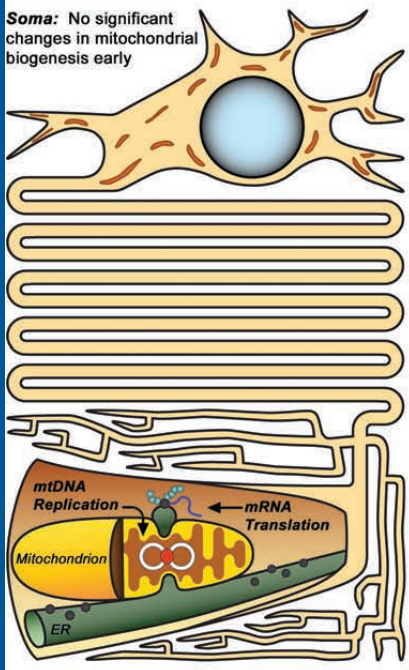

Distal Axon: Localized upregulation of mitochondrial biogenesis in response to stress-induced increases in demand; increased mitochondria in distal axons.

Later Response to Chronic Stress

Soma: Nuclear upregulation of biogenesis signals via PGC1α co-activation; increased mitochondria in soma.

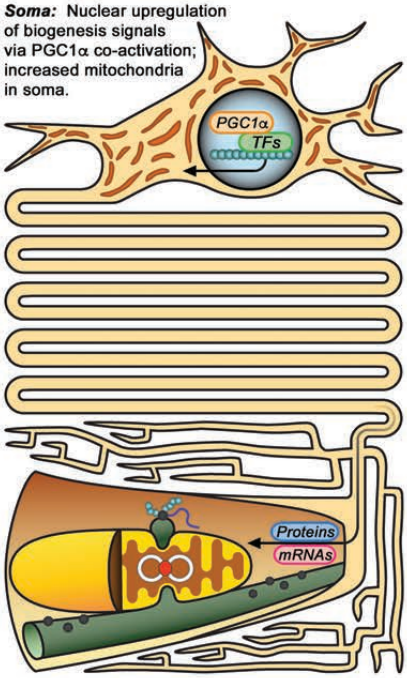

Distal Axon: Increased peripherial mitochondrial biogenesis is maintained, possibly in part by somal upregulation of resources for replication.

Pathogenic Conditions in Vulnerable Neurons

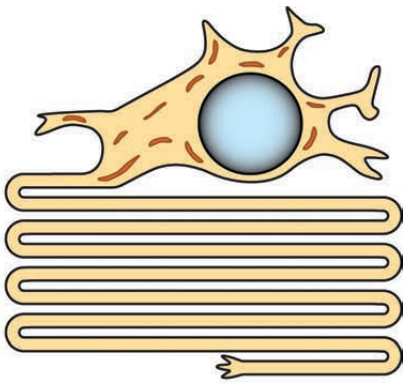

Distal Axon: Lower capacity for localized biogenesis upregulation in distal axons in response to stress may lead to bioenergetic distress and neuritic retraction ahead of cell body death.